ELSEVIER

Comput. Methods Appl. Mech. Engrg. 171 (1999) 1–23

Computer methods in applied mechanics and engineering

Global uniformly convergent finite element methods for singularly perturbed elliptic boundary value problems: higher-order elements

Jichun Li, I.M. Navon*

Department of Mathematics and Supercomputer Computations Research Institute, Florida State University, Tallahassee, FL 32306-4510, USA

Received 26 February 1998

Abstract

In this paper, we develop a general higher-order finite element method for solving singularly perturbed elliptic linear and quasilinear problems in two space dimensions. We prove that a quasioptimal global uniform convergence rate of $O(N_x^{-(m+1)} \ln^{m+1} N_x + N_y^{-(m+1)} \ln^{m+1} N_y)$ in L^2 norm is obtained for a reaction–diffusion model by using the mth order ($m \geq 2$) tensor-product element, thus answering some open problems posed by Roos in [H.-G. Roos, Layer-adapted grids for singular perturbation problems, Z. Angew. Math. Mech. 78(5) (1998) 291–309] and [H.-G. Ross, M. Stynes and L. Tobiska, Numerical Methods for Singularly Perturbed Differential Equations (Springer-Verlag, Berlin, 1996) 278]. Here, N_x and N_y are the number of partitions in the x- and y-directions, respectively. Numerical results are provided supporting our theoretical analysis.

Introduction

Recently there was great interest shown in the investigation of numerical methods for singularly perturbed problems (SPP) [2–4]. SPP arise in many areas, such as in chemical kinetics [5,6], fluid mechanics [7] and system control [8,9], etc. Usually, the solution of SPP undergoes rapid changes within very thin layers near the boundary or inside the problem domain [5,10]. These sharp transitions make SPP very difficult to solve numerically [2–4]. An extensively discussed model in fluid mechanics is the so-called 'convection dominated' problem [11–13]:

$$-\nabla \cdot \varepsilon \nabla u + c \cdot \nabla u + \sigma u = f \quad \text{in } \Omega \subseteq R^2 \tag{1}$$

$$u = 0 \quad \text{on } \partial\Omega , \tag{2}$$

where the diffusion coefficient ε is assumed to be very small in comparison with the other coefficients and $c \neq 0$. Corresponding to $c = 0$ is the so-called reaction–diffusion model. But *even if $c = 0$, the fact that ε can be very small in comparison with σ leads to notorious computational difficulties* [14, p. 310].

In this paper, we will focus on the finite element method (FEM) for solving SPP. While much work has been carried out by using many variants of FEM [11–13], few are global uniformly convergent (GUC), where the error estimate is independent of the perturbation parameter ε on the whole domain. As far as we know, a global uniform convergence can be achieved by the exponential fitted FEM [15,16,2]. However, these methods are complicated to use and have a very low convergence rate, which is only $\|u - u_h\|_\varepsilon \leq Ch^{1/2}$ for the convection–diffusion model (1), (2), where $\|w\|_\varepsilon = (\varepsilon\|\nabla w\|^2_{L^2(\Omega)} + \|w\|^2_{L^2(\Omega)})^{1/2}$. Another type of uniform convergence was

* Corresponding author. E-mail: navon@scri.fsu.edu

0045-7825/99/$ – see front matter
PII: S0045-7825(98)00243-6

achieved by *hp*-FEM. This method is very complicated and it is now only applied to some simple models, e.g. the reaction–diffusion model in one and two space dimensions [17,18]. Recently, global uniform convergence was achieved by using the standard FEM on some specially constructed piecewise uniform meshes [2,1], the so-called Shishkin mesh, which was introduced by Shishkin [19]. This type of mesh specifies a fine uniform mesh inside part of the boundary layers and a coarse uniform mesh elsewhere. Such a mesh is very easy to implement, yet it yields global uniform convergence that is independent of the perturbation parameter ε. But the known results were restricted only to the finite difference method [3] and bilinear FEM [20–24]. However, '*High-order elements seem to be more attractive than linear ones .... But precise error estimates for this technique on Shishkin meshes are still unavailable*' [1, p. 296]. Also, '*Not much is known about Shishkin-type grids for nonlinear problems*' [1, p. 297].

Our goal in this paper is to develop a general higher-order FEM, which is GUC, for solving the singularly perturbed elliptic boundary value problems in two space dimensions. To clarify the ideas, we first focus on a linear reaction–diffusion model by using a bi-quadratic finite element, where we show that our scheme is GUC in almost third order in L^2 norm. Then, a similar discussion is carried out for a quasilinear reaction–diffusion model. Some numerical results are presented, which are consistent with our theoretical analysis. A comparison was carried out between our scheme on a piecewise uniform mesh and the standard FEM on a uniform mesh. It is shown that our method performs much better than the standard FEM on the uniform mesh. Generalizations to any mth order tensor-product elements are also discussed, where $m \geqslant 3$.

Throughout the paper, we will use C (sometimes subscripted) to denote a generic constant, which is independent of the mesh size and the perturbation parameter ε. Also, we use the notation $\|\cdot\|_{\infty,\tau}$ for the L^∞ norm of τ, and $\|\cdot\|$ for the L^2 norm on Ω.

2. The 2-D linear reaction–diffusion model

In this section, we will consider the following singularly perturbed elliptic problem:

$$L_\varepsilon u \equiv -\varepsilon^2\left(\frac{\partial^2 u}{\partial x^2} + \frac{\partial^2 u}{\partial y^2}\right) + a(x, y)u = f(x, y) \quad \text{in } \Omega \equiv (0, 1)^2 , \tag{3}$$

$$u = 0 \quad \text{on } \partial\Omega , \tag{4}$$

where $0 < \varepsilon \ll 1$. The functions a and f are assumed to be sufficiently smooth in Ω and

$$a(x, y) \geqslant \alpha^2 > 0 \quad \text{in } \Omega .$$

Here, $\alpha > 0$ is a constant.

2.1. The asymptotic expansion and derivative estimates

The asymptotic expansion for (3), (4) was investigated in [25,26], from which we have:

LEMMA 2.1 [25, Theorem 2.1]. Let u solve (3), (4). There exists a constant $C_n > 0$ that is independent of ε such that

$$|u(x, y) - \tilde{u}_{2n}(x, y)| \leqslant C_n \varepsilon^{2n+1} ,$$

where

$$\tilde{u}_{2n} = U_{2n} + V_{2n} + W_{2n} + \overline{V}_{2n} + \overline{W}_{2n} + \sum_{l=1}^{4} Z^l_{2n} , \tag{5}$$

$$U_{2n}(x, y) \quad \textit{is the regular part} , \tag{6}$$

$$V_{2n}(x, \eta), W_{2n}(\xi, y), \overline{V}_{2n}(x, \overline{\eta}), \overline{W}_{2n}(\overline{\xi}, y) \quad \textit{are the boundary layer functions} , \tag{7}$$

$$Z^1_{2n}(\xi, \eta), Z^2_{2n}(\overline{\xi}, \eta), Z^3_{2n}(\xi, \overline{\eta}), Z^4_{2n}(\overline{\xi}, \overline{\eta}) \quad \textit{are the corner layer functions} . \tag{8}$$

Here, $\xi = x/\varepsilon$, $\eta = y/\varepsilon$, $\bar{\xi} = (1-x)/\varepsilon$, $\bar{\eta} = (1-y)/\varepsilon$. *Also, the following estimates hold true:*

$$|V_{2n}(x, \eta)| \leq C_m \, e^{-\alpha\eta} , \tag{9}$$

$$\|W_{2n}(\xi, y)| \leq C_m \, e^{-\alpha\xi} , \tag{10}$$

$$|\bar{V}_{2n}(x, \bar{\eta})| \leq C_m \, e^{-\alpha\bar{\eta}} , \tag{11}$$

$$|\bar{W}_{2n}(\bar{\xi}, y)| \leq C_m \, e^{-\alpha\bar{\xi}} , \tag{12}$$

$$|Z^1_{2n}(\xi, \eta)| \leq C \, e^{-\alpha(\xi+\eta)} , \tag{13}$$

$$|Z^2_{2n}(\bar{\xi}, \eta)| \leq C \, e^{-\alpha(\bar{\xi}+\eta)} , \tag{14}$$

$$|Z^3_{2n}(\xi, \bar{\eta})| \leq C \, e^{-\alpha(\xi+\bar{\eta})} , \tag{15}$$

$$|Z^4_{2n}(\bar{\xi}, \bar{\eta})| \leq C \, e^{-\alpha(\bar{\xi}+\bar{\eta})} . \tag{16}$$

From Lemmas 3.1, 3.3 and 3.5 of [22], we have

LEMMA 2.2. For the solution u of (3), (4), we have

$$\text{(I)} \quad |u_{x^n}(x, y)| \leq C(1 + \varepsilon^{-n} \, e^{-\alpha x}{}_{\varepsilon} + \varepsilon^{-n} \, e^{-\alpha(1-x)}{}_{\varepsilon}) \quad \text{on } \bar{\Omega} \equiv \Omega \cup \partial\Omega , \tag{17}$$

$$\text{(II)} \quad |u_{y^n}(x, y)| \leq C(1 + \varepsilon^{-n} \, e^{-\alpha y}{}_{\varepsilon} + \varepsilon^{-n} \, e^{-\alpha(1-y)}{}_{\varepsilon}) \quad \text{on } \bar{\Omega} , \tag{18}$$

where $n = 0, 1, 2$.

In order to use higher-order FEM, we need to obtain higher-order derivative estimates for the solution of (3), (4). By using the boundary condition (4) in (3), we have

$$u_{xx}|_{x=0} = -\varepsilon^{-2} f(0, y) , \qquad u_{xx}|_{x=1} = -\varepsilon^{-2} f(1, y) \tag{19}$$

$$u_{xx}|_{y=0} = u_{xx}|_{y=1} = 0 \tag{20}$$

or in one simple form as

$$u_{xx}(x, y) = g(x, y, \varepsilon) \quad \text{on } \partial\Omega ,$$

where $g(x, y, \varepsilon) = -\varepsilon^{-2}(1-x)f(0, y) - \varepsilon^{-2}xf(1, y)$. Here, the compatibility conditions [25]

$$f(0, 0) = f(0, 1) = f(1, 0) = f(1, 1) = 0$$

were used.

By denoting $\tilde{u}(x, y) = u_{xx}(x, y) - g(x, y, \varepsilon)$, and differentiating (3) twice with respect to x, we have

$$L_\varepsilon \tilde{u} \equiv -\varepsilon^2 \, \Delta\tilde{u} + a\tilde{u} = \tilde{F} \quad \text{in } \Omega , \tag{21}$$

$$\tilde{u} = 0 \quad \text{on } \partial\Omega , \tag{22}$$

where $\tilde{F} = f_{xx} - 2a_x u_x - a_{xx} u + \varepsilon^2 g_{xx} + \varepsilon^2 g_{yy} - ag$.

LEMMA 2.3.

$$\text{(I)} \quad |\tilde{u}_x(x, y)| \leq C\varepsilon^{-3} , \quad \text{on } \partial\Omega \tag{23}$$

$$\text{(II)} \quad |\tilde{u}_y(x, y)| \leq C\varepsilon^{-3} , \quad \text{on } \partial\Omega \tag{24}$$

PROOF. Using the barrier function

$$\phi = C\varepsilon^{-2}(1 - e^{-\alpha x/\varepsilon})(1 - e^{-\alpha(1-x)/\varepsilon}) ,$$

and after some simple calculations, we have

$$L_\varepsilon(\phi\pm\tilde{u}) = \frac{C\alpha^2}{\varepsilon^2}[e^{-\alpha x/\varepsilon} + e^{-\alpha(1-x)/\varepsilon}] + \frac{Ca}{\varepsilon^2}(1-e^{-\alpha x/\varepsilon})(1-e^{-\alpha(1-x)/\varepsilon})\pm\tilde{F} \tag{25}$$

$$\geqslant \frac{C\alpha^2}{\varepsilon^2}(1+e^{-\alpha/\varepsilon})\pm\tilde{F} \tag{26}$$

$$\geqslant 0\,, \quad \text{for sufficiently large } C\,, \tag{27}$$

where we used the fact that $a \geqslant \alpha^2$ and $|\tilde{F}| \leqslant C_1\varepsilon^{-2}$.

Hence, by using the maximum principle [22, Theorem 3.1] and the fact that

$$(\phi\pm\tilde{u})|_{\partial\Omega} \geqslant 0\,,$$

we obtain

$$|\tilde{u}| \leqslant \phi = C\varepsilon^{-2}(1-e^{-\alpha x/\varepsilon})(1-e^{-\alpha(1-x)/\varepsilon})\,, \quad \text{on } \bar{\Omega} \tag{28}$$

from which we have

$$|\tilde{u}_x(0,y)| = \left|\lim_{x\to 0^+}\frac{\tilde{u}(x,y)-\tilde{u}(0,y)}{x}\right| \leqslant \lim_{x\to 0^+}\left|\frac{\tilde{u}(x,y)-\tilde{u}(0,y)}{x}\right| \tag{29}$$

$$\leqslant \lim_{x\to 0^+}\frac{C\varepsilon^{-2}(1-e^{-\alpha x/\varepsilon})(1-e^{-\alpha(1-x)/\varepsilon})}{x} \leqslant \alpha C\varepsilon^{-3}\,. \tag{30}$$

Similarly,

$$|\tilde{u}_x(1,y)| \leqslant \lim_{x\to 1^-}\left|\frac{\tilde{u}(1,y)-\tilde{u}(x,y)}{1-x}\right| \leqslant C\varepsilon^{-3}\,.$$

From the boundary condition (22), we have

$$\tilde{u}_x(x,0) = 0 = \tilde{u}_x(x,1)\,.$$

By combining the above inequalities, we obtain

$$|\tilde{u}_y(x,y)|_{\partial\Omega} \leqslant C\varepsilon^{-3} \tag{31}$$

By symmetry, we can easily obtain

$$|\tilde{u}_y(x,y)|_{\partial\Omega} \leqslant C\varepsilon^{-3}$$

which along with (31) concludes our proof. □

LEMMA 2.4.

$$(I)\quad |u_{x^3}(x,y)| \leqslant C\varepsilon^{-3}\,, \quad \text{on } \bar{\Omega} \tag{32}$$

$$(II)\quad |u_{y^3}(x,y)| \leqslant C\varepsilon^{-3}\,, \quad \text{on } \bar{\Omega} \tag{33}$$

PROOF. Consider the barrier function $\phi = C\varepsilon^{-3}$, then we have

$$L_\varepsilon(\phi\pm\tilde{u}_x) = \alpha C\varepsilon^{-3}\pm(\tilde{F}_x - a_x\tilde{u}) \tag{34}$$

$$\geqslant 0\,, \quad \text{for sufficiently large } C\,. \tag{35}$$

By Lemma 2.3, we obtain

$$(\phi\pm\tilde{u}_x)|_{\partial\Omega} \geqslant 0$$

from which together with the maximum principle [22, Theorem 3.1], we have

$$|\tilde{u}_x(x,y)| \leq \phi = C\varepsilon^{-3}, \quad \text{on } \bar{\Omega}.$$

Hence, by the definition of $\tilde{u}$, we have

$$|u_{x^3}(x,y)| = |(\tilde{u}+g)_x| \leq C\varepsilon^{-3}$$

which concludes the proof of (I).

The proof of (II) can be carried out similarly. □

2.2. The mesh and the finite element scheme

Since our problem has boundary layers located along all sides of the rectangle Ω, our piecewise uniform mesh can be constructed in the same way as we did in [22].

Assume that the positive integers N_x and N_y are divisible by 4, where N_x and N_y denote the number of elements in the x- and y-directions, respectively. In the x-direction, we first divide the interval [0, 1] into the subintervals

$$[0, \sigma_x], \quad [\sigma_x, 1-\sigma_x], \quad [1-\sigma_x, 1].$$

Uniform meshes are then used on each subinterval, with $N_x/4$ points on each of $[0, \sigma_x]$ and $[1-\sigma_x, 1]$, and $N_x/2$ points on $[\sigma_x, 1-\sigma_x]$, where $\sigma_x = 3\alpha^{-1}\varepsilon \ln N_x$. Here, for simplicity, we assume that $\sigma_x \leq 1/4$, since we are considering SPP where ε is very small.

In the y-direction, we follow the same method described above by dividing the interval [0, 1] into the subintervals

$$[0, \sigma_y], \quad [\sigma_y, 1-\sigma_y], \quad [1-\sigma_y, 1].$$

Uniform meshes are then used on each subinterval, with $N_y/4$ points on each of $[0, \sigma_y]$ and $[1-\sigma_y, 1]$, and $N_y/2$ points on $[\sigma_y, 1-\sigma_y]$, where $\sigma_y = 3\alpha^{-1}\varepsilon \ln N_y$.

Let $I_i = [x_{i-1}, x_i]$, $I = [0, 1]$, $\tilde{I}_i = I_i \times I$, $h = \max_{1\leq i\leq N_x} h_i$, $K_j = [y_{j-1}, y_j]$, $\tilde{K}_j = I \times K_j$ and $k = \max_{1\leq j\leq N_y} k_j$. Here, $h_i = x_i - x_{i-1}$ and $k_j = y_j - y_{j-1}$.

The weak formulation of (3), (4) is: Find $u \in H_0^1(\Omega)$ such that

$$B(u,v) \equiv \varepsilon^2(\nabla u, \nabla v) + (au, v) = (f, v), \quad \forall v \in H_0^1(\Omega), \tag{36}$$

where $(\cdot,\cdot)$ denotes the usual $L^2(\Omega)$ inner product and $H_0^1(\Omega)$ is the usual Sobolev space.

Denote the weighted energy norm

$$|||v||| \equiv \{\varepsilon^2\|\nabla v\|^2 + \|v\|^2\}^{1/2}, \quad \forall v \in H_0^1(\Omega).$$

Also, we have

$$B(v,v) = \varepsilon^2\|\nabla v\|^2 + (av, v) \geq \min\{1, \alpha^2\}|||v|||^2. \tag{37}$$

Let $S_h(\Omega)$ be the ordinary tensor–product quadratic element space, and

$$\Pi w = \Pi_x\Pi_y w = \Pi_y\Pi_x w$$

be the bi-quadratic interpolation of w, where Π_x and Π_y are the interpolations in the x- and y-directions, respectively. More explicitely, the one-dimensional interpolation Π_x on $[x_{i-1}, x_i]$ can be written as

$$\Pi_x w(x) = w(x_{i-1})\psi_1(\xi) + w\left(\frac{x_{i-1}+x_i}{2}\right)\psi_2(\xi) + w(x_i)\psi_3(\xi), \tag{38}$$

where the shape functions are [27, p. 67]

$$\psi_1(\xi) = -\frac{1}{2}\xi(1-\zeta) \tag{39}$$

$$\psi_2(\xi) = (1+\xi)(1-\xi) \tag{40}$$

$$\psi_3(\xi) = \frac{1}{2}\,\xi(1+\xi) \tag{41}$$

Here, the transformation $\xi = (2x - (x_{i-1} + x_i))/(x_i - x_{i-1})$ maps $[x_{i-1}, x_i]$ to $[-1, 1]$.
From (38), we have

$$\|\Pi_x w\|_{\infty,I_i} \leqslant \|w\|_{\infty,I_i} \cdot \max_{-1\leqslant\xi\leqslant 1} (|\psi_1(\xi)| + |\psi_2(\xi)| + |\psi_3(\xi)|) \tag{42}$$

$$\leqslant \|w\|_{\infty,I_i} \cdot \max_{-1\leqslant\xi\leqslant 1} \left[\frac{1}{2}|\xi|(1-\xi) + (1-\xi^2) + \frac{1}{2}|\xi|(1+\xi)\right] \tag{43}$$

$$\leqslant 2\|w\|_{\infty,I_i} \tag{44}$$

Hence, we obtain

LEMMA 2.5.

(1) $\Pi w = \Pi_x \Pi_y w = \Pi_y \Pi_x w$ (45)

(2) $\|\Pi_x w\|_{\infty,\bar{I}_i} \leqslant 2\|w\|_{\infty,\bar{I}_i}$ (46)

(3) $\|w - \Pi_x w\|_{\infty,\bar{I}_i} \leqslant \frac{1}{48} h_i^3 \|w_{x^3}|_{\infty,\bar{I}_i}$ (47)

Similar results hold true for the interpolation Π_y.

PROOF.
(1) Use the definition of the bi-quadratic interpolation.
(2) By (44).
(3) By [27, p. 73].
We seek the finite element solution $u_h \in S_h(\Omega)$ such that

$$B(u_h, v_h) \equiv \varepsilon^2(\nabla u_h, \nabla v_h) + (au_h, v_h) = (f, v_h)\,, \quad \forall\, v_h \in S_h(\Omega) \quad \square\,. \tag{48}$$

2.3. Main results

Using the techniques used in [21–24], we can obtain the following interpolation estimates:

LEMMA 2.6. For the solution u of (3), (4) and for any integer $n \geqslant 0$, *we have*

(I) $\|u - \Pi_x u\|_{\infty,\bar{I}_i} \leqslant C(N_x^{-3} \ln^3 N_x + \varepsilon^{2n+1})$ (49)

(II) $\|u - \Pi_y u\|_{\infty,\bar{K}_j} \leqslant C(N_y^{-3} \ln^3 N_y + \varepsilon^{2n+1})$ (50)

PROOF. For $i = 1, \ldots, i_0, N_x - i_0 + 1, \ldots, N_x$, by Lemmas 2.5 and 2.4, we have

$$\begin{aligned}\|u - \Pi_x u\|_{\infty,\bar{I}_i} &\leqslant Ch_i^3 \|u_{x^3}\|_{\infty,\bar{I}_i} \leqslant Ch_i^3 \varepsilon^{-3}\\ &\leqslant CN_x^{-3} \ln^3 N_x\,,\end{aligned}$$

since $h_i = 4\sigma_x/N_x = 12\alpha^{-1}\varepsilon N_x^{-1} \ln N_x$ in this case. Hence, (I) is true in this case.
For $i = i_0 + 1, \ldots, N_x - i_0$, in this case $[x_{i-1}, x_i] \subseteq [\sigma_x, 1 - \sigma_x]$. Note that

$$u - \Pi_x u = (u - \tilde{u}_{2n}) - \Pi_x(u - \tilde{u}_{2n}) + (\tilde{u}_{2n} - \Pi_x \tilde{u}_{2n}) \tag{51}$$

By Lemmas 2.5 and 2.1, we obtain

$$\|(u - \tilde{u}_{2n}) - \Pi_x(u - \tilde{u}_{2n})\|_{\infty,\bar{I}_i} \leqslant 3\|u - \tilde{u}_{2n}\|_{\infty,\bar{I}_i} \leqslant C\varepsilon^{2n+1} \tag{52}$$

By using the asymptotic expansion and the exponentially decaying estimates of Lemma 2.1, we can obtain the estimate of $\tilde{u}_{2n} - \Pi_x \tilde{u}_{2n}$ in the same way as we did in [22,23]. Explicitly, we have

$$\|\tilde{u}_{2n} - \Pi_x \tilde{u}_{2n}\|_{\infty,\bar{I}_i} \leq C N_x^{-3} \tag{53}$$

Combining (51)–(53), we see that (I) holds true in this case, which concludes our proof of (I). The proof of (II) can be carried out in a similar manner. □

Therefore, we have

LEMMA 2.7. For the solution u of (3), (4) and any integer $n \geq 0$, we have

$$\|u - \Pi u\|_{\infty,\bar{\Omega}} \leq C(N_x^{-3} \ln^3 N_x + N_y^{-3} \ln^3 N_y + \varepsilon^{2n+1}).$$

PROOF. By Lemmas 2.5 and 2.6, we have

$$\|u - \Pi u\|_{\infty,\bar{\Omega}} \leq \|u - \Pi_x u\|_{\infty,\bar{\Omega}} + \|\Pi_x(u - \Pi_y u)\|_{\infty,\bar{\Omega}} \tag{54}$$

$$\leq \|u - \Pi_x u\|_{\infty,\bar{\Omega}} + 2\|u - \Pi_y u\|_{\infty,\bar{\Omega}} \tag{55}$$

$$\leq \max_{1 \leq i \leq N_x} \|u - \Pi_x u\|_{\infty,\bar{I}_i} + 2 \max_{1 \leq j \leq N_y} \|u - \Pi_y u\|_{\infty,\bar{K}_j} \tag{56}$$

$$\leq C(N_x^{-3} \ln^3 N_x + N_y^{-3} \ln^3 N_y + \varepsilon^{2n+1}) \tag{57}$$

which concludes our proof. □

THEOREM 2.1.

$$\|u - u_h\| \leq C(1 + \varepsilon N_x + \varepsilon^{1/2} N_x \ln^{-1/2} N_x + \varepsilon N_y + \varepsilon^{1/2} N_y \ln^{-1/2} N_y)\|u - \Pi u\|_{\infty,\bar{\Omega}}$$

PROOF. Note that

$$C_1 |\!|\!| \Pi u - u_h |\!|\!|^2 \leq B(\Pi u - u_h, \Pi u - u_h) = B(\Pi u - u, \Pi u - u_h) \tag{58}$$

$$= \varepsilon^2(\nabla(\Pi u - u), \nabla\chi) + (a(\Pi u - u), \chi) \tag{59}$$

where here and in the following, we will use the notation $\chi \equiv \Pi u - u_h$.

Integrating by parts, we obtain

$$\varepsilon^2((\Pi u - u)_x, \chi_x) = \sum_{1 \leq i \leq N_x, 1 \leq j \leq N_y} \int_{x_{i-1}}^{x_i} \int_{y_{j-1}}^{y_j} \varepsilon^2(\Pi u - u)_x \chi_x \, dx \, dy$$

$$= \sum_{1 \leq i \leq N_x, 1 \leq j \leq N_y} \int_{y_{j-1}}^{y_j} [\varepsilon^2(\Pi u - u)\chi_x]|_{x=x_{i-1}}^{x=x_i} \, dy - \varepsilon^2(\Pi u - u, \chi_{xx})$$

$$\leq \varepsilon\|\Pi u - u\|_{\infty,\bar{\Omega}} \sum_{1 \leq i \leq N_x, 1 \leq j \leq N_y} \int_{y_{j-1}}^{y_j} [|\varepsilon\chi_x(x_i, y)| + |\varepsilon\chi_x(\chi_{i-1}, y)|] \, dy$$

$$+ \sum_{1 \leq i \leq N_x, 1 \leq j \leq N_y} \int_{x_{i-1}}^{x_i} \int_{y_{j-1}}^{y_j} |\varepsilon^2(\Pi u - u)\chi_{xx}| \, dy \, dx$$

By using the Taylor expansion and the fact that χ is a quadratic function in x, we have

$$\sum_{1\le i\le N_x, 1\le j\le N_y} \int_{y_{j-1}}^{y_j} |\varepsilon\chi_x(x_i, y)|\,dy = \sum_{i,j} \frac{1}{x_i - x_{i-1}} \int_{x_{i-1}}^{x_i}\int_{y_{j-1}}^{y_j} |\varepsilon\chi_x(x_i, y)|\,dy\,dx$$
$$= \sum_{i,j} \frac{1}{x_i - x_{i-1}} \int_{x_{i-1}}^{x_i}\int_{y_{j-1}}^{y_j} |\varepsilon\chi_x(x, y) + (x_i - x)\varepsilon\chi_{xx}(x, y)|\,dy\,dx$$
$$\le \sum_{i,j} \left[\frac{1}{x_i - x_{i-1}} \int_{x_{i-1}}^{x_i}\int_{y_{j-1}}^{y_j} |\varepsilon\chi_x|\,dy\,dx + \int_{x_{i-1}}^{x_i}\int_{y_{j-1}}^{y_j} |\varepsilon\chi_{xx}|\,dy\,dx\right]$$

where $\Sigma_{i,j}$ is a short hand notation for $\Sigma_{1\le i\le N_x, 1\le j\le N_y}$.

Note that

$$\sum_{i,j} \frac{1}{x_i - x_{i-1}} \int_{x_{i-1}}^{x_i}\int_{y_{j-1}}^{y_j} |\varepsilon\chi_x|\,dy\,dx \le CN_x \int_{S_1} |\varepsilon\chi_x|\,dy\,dx + \frac{CN_x}{\varepsilon \ln N_x} \int_{S_2} |\varepsilon\chi_x|\,dy\,dx$$
$$\le CN_x(\text{meas}(S_1))^{1/2}\|\varepsilon\chi_x\|_{L^2(S_1)} + \frac{CN_x}{\varepsilon \ln N_x}(\text{meas}(S_2))^{1/2}\|\varepsilon\chi_x\|_{L^2(S_2)}$$
$$\le CN_x\|\varepsilon\chi_x\|_{L^2(S_1)} + C\frac{N_x}{\varepsilon \ln N_x}(\varepsilon \ln N_x)^{1/2}\|\varepsilon\chi_x\|_{L^2(S_2)}$$
$$\le C(N_x + \varepsilon^{-1/2} N_x \ln^{-1/2} N_x)\|\varepsilon\chi_x\|$$

where $S_1 \equiv [\sigma_x, 1-\sigma_x] \times [0, 1]$ and $S_2 \equiv \bar{\Omega}\backslash S_1$.

In the same way, we can obtain

$$\sum_{i,j} \int_{y_{j-1}}^{y_j} |\varepsilon\chi_x(x_{i-1}, y)|\,dy \le C(N_x + \varepsilon^{-1/2} N_x \ln^{-1/2} N_x)\|\varepsilon\chi_x\| \tag{60}$$

Similarly, we have

$$\sum_{i,j} \int_{x_{i-1}}^{x_i}\int_{y_{j-1}}^{y_j} |\varepsilon\chi_{xx}|\,dy\,dx = \int_{S_1} |\varepsilon\chi_{xx}|\,dy\,dx + \int_{S_2} |\varepsilon\chi_{xx}|\,dy\,dx$$
$$\le (\text{meas}(S_1))^{1/2}\|\varepsilon\chi_{xx}\|_{L^2(S_1)} + (\text{meas}(S_2))^{1/2}\|\varepsilon\chi_{xx}\|_{L^2(S_2)}$$
$$\le \|\varepsilon\chi_{xx}\|_{L^2(S_1)} + C(\varepsilon \ln N_x)^{1/2}\|\varepsilon\chi_{xx}\|_{L^2(S_2)}$$
$$\le CN_x\|\varepsilon\chi_x\|_{L^2(S_1)} + C(\varepsilon \ln N_x)^{1/2}\frac{N_x}{\varepsilon \ln N_x}\|\varepsilon\chi_x\|_{L^2(S_2)}$$
$$\le C(N_x + \varepsilon^{-1/2} N_x \ln^{-1/2} N_x)\|\varepsilon\chi_x\| \tag{61}$$

where we used the standard inverse estimate [28, Section 4.5]

$$\|\chi_{xx}\| \le Ch^{-1}\|\chi_x\|, \quad \forall\, \chi \in S_h(\Omega)$$

and the fact that

$$h = O(N_x^{-1}) \quad \text{and} \quad h = O(\varepsilon N_x^{-1} \ln N_x) \quad \text{on } S_2\,.$$

On the other hand,

$$\sum_{i,j} \int_{x_{i-1}}^{x_i}\int_{y_{j-1}}^{y_j} \varepsilon^2(\Pi u - u)\chi_{xx}\,dy\,dx \le C\varepsilon\|\Pi u - u\|_{\infty,\bar{\Omega}}\left[\int_{S_1} |\varepsilon\chi_{xx}|\,dy\,dx + \int_{S_2} |\varepsilon\chi_{xx}|\,dy\,dx\right]$$
$$\le C\varepsilon\|\Pi u - u\|_{\infty,\bar{\Omega}}(N_x + \varepsilon^{-1/2} N_x \ln^{-1/2} N_x)\|\varepsilon\chi_x\|$$

where we used (61).

By combining the above inequalities, we have

$$\varepsilon^2((\Pi u - u)_x, \chi_x) \le C(\varepsilon N_x + \varepsilon^{1/2} N_x \ln^{-1/2} N_x)\|\Pi u - u\|_{\infty,\bar{\Omega}}\|\varepsilon\chi_x\| \tag{62}$$

In the same way, we can obtain

$$\varepsilon^2((\Pi u - u)_y, \chi_y) \leq C(\varepsilon N_y + \varepsilon^{1/2} N_y \ln^{-1/2} N_y)\|\Pi u - u\|_{\infty,\bar{\Omega}} \|\varepsilon \chi_y\| \tag{63}$$

Finally, we have

$$|(a(\Pi u - u), \chi)| \leq C\|\Pi u - u\|_{\infty,\bar{\Omega}} \|\chi\| \tag{64}$$

By combining the inequalities (58)–(64), we have

$$|\!|\!|\Pi u - u_h|\!|\!| \leq C(1 + \varepsilon N_x + \varepsilon^{1/2} N_x \ln^{-1/2} N_x + \varepsilon N_y + \varepsilon^{1/2} N_y \ln^{-1/2} N_y)\|\Pi u - u\|_{\infty,\bar{\Omega}}$$

from which together with the triangular inequality, we obtain

$$\begin{aligned} \|u - u_h\| &\leq \|u - \Pi u\| + \|\Pi u - u_h\| \\ &\leq C(1 + \varepsilon N_x + \varepsilon^{1/2} N_x \ln^{-1/2} N_x + \varepsilon N_y + \varepsilon^{1/2} N_y \ln^{-1/2} N_y)\|\Pi u - u\|_{\infty,\bar{\Omega}} \end{aligned}$$

which concludes our proof. □

From Theorem 2.1, we see that under the assumption:

(A3) $\varepsilon \leq \max(N_x^{-2} \ln N_x, N_y^{-2} \ln N_y)$,

the error $\|u - u_h\|$ is bounded by the interpolation error $\|u - \Pi u\|_{\infty,\bar{\Omega}}$. By Lemma 2.7, if the solution u is smooth enough, then the interpolation estimate will be dominated by $N_x^{-3} \ln^3 N_x + N_y^{-3} \ln^3 N_y$, in which case we can obtain the following quasi-optimal global uniformly convergent result:

THEOREM 2.2. Let u be the solution of (3), (4), u_h be the bi-quadratic finite element solution of (48). Then, under the assumption (A3), we have

$$\|u - u_h\| \leq C(N_x^{-3} \ln^3 N_x + N_y^{-3} \ln^3 N_y).$$

2.4. Generalizations to any mth order tensor–product elements

If the solution u of (1), (2) is smooth enough, we can use higher-order elements to find the finite element solution u_h of (48) in the mth order ($m \geq 3$) tensor–product element space $S_h(\Omega)$, where $S_h(\Omega)$ can be constructed in the same way as the bi-quadratic element except that

$$\sigma_x = (m+1)\alpha^{-1} \varepsilon \ln N_x \quad \text{and} \quad \sigma_y = (m+1)\alpha^{-1} \varepsilon \ln N_y$$

for the mth order tensor–product element, in which case, we have the following quasi-optimal global uniform convergence:

THEOREM 2.3. Let u be the solution of (3), (4), u_h be the finite element solution of (48) on the mth order ($m \geq 3$) tensor–product element space. Then, using the assumption (A3), we have

$$\|u - u_h\| \leq C(N_x^{-(m+1)} \ln^{m+1} N_x + N_y^{-(m+1)} \ln^{m+1} N_y).$$

The proof of this theorem can be obtained by carrying out similar proofs as for the bi-quadratic case. Hence, in the following, we will just sketch out some critical steps.

By carrying out the same techniques used in Lemmas 2.3 and 2.4, we can easily obtain

LEMMA 2.8.

$$\text{(I)} \quad |u_{x^{m+1}}(x, y)| \leq C\varepsilon^{-(m+1)}, \quad \text{on } \bar{\Omega} \tag{65}$$

$$\text{(II)} \quad |u_{y^{m+1}}(x, y)| \leq C\varepsilon^{-(m+1)}, \quad \text{on } \bar{\Omega} \tag{66}$$

Also, we have

LEMMA 2.9. For the mth order ($m \geqslant 3$) tensor-product interpolation Π, we have

$$\text{(I)} \quad \Pi w = \Pi_x \Pi_y w = \Pi_y \Pi_x w \tag{67}$$

$$\text{(II)} \quad \|\Pi_x w\|_{\infty,\bar{I}_i} \leqslant C_m \|w\|_{\infty,\bar{I}_i} \tag{68}$$

$$\text{(III)} \quad \|w - \Pi_x w\|_{\infty,\bar{I}_i} \leqslant \frac{h_i^{m+1}}{2^{m+1} \cdot (m+1)!} \|w_{x^{m+1}}\|_{\infty,\bar{I}_i} \tag{69}$$

where C_m is a constant depending on m. Similar results hold true for the interpolation Π_y.

PROOF.

(I) By the definition of the tensor-product interpolation.

(II) For simplicity, hereby we just provide here the proof for the bi-cubic element, in which case the one-dimensional shape functions [27, Section 2.6] are

$$\psi_1(\xi) = -\frac{9}{16}(1-\xi)\left(\frac{1}{3}-\xi\right)\left(\frac{1}{3}+\xi\right) \tag{70}$$

$$\psi_2(\xi) = \frac{27}{16}(1+\xi)(1-\xi)\left(\frac{1}{3}-\xi\right) \tag{71}$$

$$\psi_3(\xi) = \frac{27}{16}(1+\xi)(1-\xi)\left(\frac{1}{3}+\xi\right) \tag{72}$$

$$\psi_4(\xi) = -\frac{9}{16}(1+\xi)\left(\frac{1}{3}-\xi\right)\left(\frac{1}{3}+\xi\right) \tag{73}$$

Hence, we have

$$\|\Pi_x w\|_{\infty,\bar{I}_i} \leqslant \|w\|_{\infty,\bar{I}_i} \max_{-1 \leqslant \xi \leqslant 1} [|\psi_1(\xi)| + |\psi_2(\xi)| + |\psi_3(\xi)| + |\psi_4(\xi)|] \tag{74}$$

$$\leqslant \|w\|_{\infty,\bar{I}_i} \max_{-1 \leqslant \xi \leqslant 1} \left[\frac{9}{16}(1-\xi)\left|\frac{1}{9}-\xi^2\right|\right. \tag{75}$$

$$\left. + \frac{27}{16}(1-\xi^2)\left|\frac{1}{3}-\xi\right| + \frac{27}{16}(1-\xi^2)\left|\frac{1}{3}+\xi\right| + \frac{9}{16}(1+\xi)\left|\frac{1}{9}-\xi^2\right|\right] \tag{76}$$

$$\leqslant \|w\|_{\infty,\bar{I}_i}\left[\frac{9}{16}\cdot 2\cdot\frac{8}{9} + \frac{27}{16}\cdot\frac{4}{3} + \frac{27}{16}\cdot\frac{4}{3} + \frac{9}{16}\cdot 2\cdot\frac{8}{9}\right] \tag{77}$$

$$= 6.5\|w\|_{\infty,\bar{I}_i} \tag{78}$$

from which we see $C_3 = 6.5$.

For the general case, $C_m = \max_{-1 \leqslant \xi \leqslant 1} \Sigma_{i=1}^{m+1} |\psi_i(\xi)|$, where $\{\psi_i(\xi)\}_{i=1}^{m+1}$ are the one-dimensional mth order shape functions [27, Section 2.6].

(III) By [27, p. 73].

By using a similar proof of Lemmas 2.6 and 2.7, we can easily obtain

LEMMA 2.10. For the solution u of (3), (4) and any integer $n \geqslant 0$, we have

$$\|u - \Pi u\|_{\|\infty,\bar{\Omega}} \leqslant C(N_x^{-(m+1)} \ln^{m+1} N_x + N_y^{-(m+1)} \ln^{m+1} N_y + \varepsilon^{2n+1}) .$$

It is not difficult to see that Theorem 2.1 holds true for the mth order ($m \geqslant 3$) tensor-product element. The proof is almost the same. The only difference occurs in dealing with the terms

$$\sum_{i,j} \int_{y_{j-1}}^{y_j} |\varepsilon \chi_x(x_i, y)| \, dy \quad \text{and} \quad \sum_{i,j} \int_{y_{j-1}}^{y_j} |\varepsilon \chi_x(x_{i-1}, y)| \, dy .$$

In the present case, we need a Taylor expansion up to the mth order, since χ is a mth order function in x. Hence, we have

$$\sum_{i,j} \int_{y_{j-1}}^{y_j} |\varepsilon \chi_x(x_i, y)| \,dy = \sum_{i,j} \frac{1}{x_i - x_{i-1}} \int_{x_{i-1}}^{x_i} \int_{y_{j-1}}^{y_j} |\varepsilon \chi_x(x_i, y)| \,dy\,dx$$
$$= \sum_{i,j} \frac{1}{x_i - x_{i-1}} \int_{x_{i-1}}^{x_i} \int_{y_{j-1}}^{y_j} \left| \varepsilon \chi_x(x, y) + \sum_{l=1}^{m-1} \frac{(x_i - x)^l}{l!} \varepsilon \chi_{x^{l+1}}(x, y) \right| \,dy\,dx$$
$$\leq \sum_{i,j} \left[\frac{1}{x_i - x_{i-1}} \int_{x_{i-1}}^{x_i} \int_{y_{j-1}}^{y_j} |\varepsilon \chi_x| \,dy\,dx + C \int_{x_{i-1}}^{x_i} \int_{y_{j-1}}^{y_j} |\varepsilon \chi_{xx}| \,dy\,dx \right]$$

where in the last step, we used the standard inverse estimate

$$\|\chi_{x^{l+1}}\| \leq C h^{1-l} \|\chi_{xx}\|, \quad \forall \chi \in S_h(\Omega).$$

By combining Lemmas 2.8–2.10 and Theorem 2.1, we conclude the proof of Theorem 2.3. □

3. The 2-D quasilinear reaction–diffusion model

In this section, we will consider the following quasilinear singularly perturbed elliptic problem:

$$\varepsilon^2 \Delta u = F(u, x, y), \quad \text{in } \Omega = (0, 1) \times (0, 1) \tag{79}$$

$$u = 0 \quad \text{on } \partial\Omega. \tag{80}$$

The asymptotic expansion for this problem was constructed by Denisov [29], where F was assumed to be in the form of $A(u^2 + pu + q)$. For simplicity, the following conditions are assumed [29, p. 1342]:

(A1) The equation $F(u, x, y) = 0$ has a solution $u = \bar{u}_0(x, y)$ in $\bar{\Omega}$.

(A2) The derivative of F satisfies $m_2 \geq F_u(u, x, y) \geq m_1 > 0$ in $\bar{\Omega}$.

Under the above assumptions, we have:

LEMMA 3.1 [29, Section 4]. Denote the nth order asymptotic expansion

$$U_n(x, y, \varepsilon) = \sum_{k=0}^{n} \varepsilon^k (\bar{u}_k + \Pi_k^{(1)} + \cdots + \Pi_k^{(4)} + P_k^{(1)} + \cdots + P_k^{(4)}) \tag{81}$$

Then, we have

$$\max_{\bar{\Omega}} |u(x, y, \varepsilon) - U_n(x, y, \varepsilon)| = O(\varepsilon^{n+1}) \quad \text{as } \varepsilon \to 0, \tag{82}$$

where

$\bar{u}_k(x, y)$ *is the regular part of the asymptotic expansion,*

$\Pi^{(1)}(x, \eta), \Pi^{(2)}(\xi, y), \Pi^{(3)}(x, \eta_*), \Pi^{(4)}(\xi_*, y)$ *are the boundary layer functions,*

$P^{(1)}(\xi, \eta), P^{(2)}(\xi, \eta_*), P^{(3)}(\xi_*, \eta_*), P^{(4)}(\xi_*, \eta)$ *are the corner layer functions.*

Here, $\eta = y/\varepsilon$, $\xi = x/\varepsilon$, $\eta_* = (1-y)/\varepsilon$, $\xi_* = (1-x)/\varepsilon$. *Also, the following estimates hold true:*

$$|\Pi^{(1)}(x, \eta)| \leq C\,e^{-\alpha\eta},$$
$$|\Pi^{(2)}(\xi, y)| \leq C\,e^{-\alpha\xi},$$
$$|\Pi^{(3)}(x, \eta_*)| \leq C\,e^{-\alpha\eta_*},$$
$$|\Pi^{(4)}(\xi_*, y)| \leq C\,e^{-\alpha\xi_*},$$
$$|P^{(1)}(\xi, \eta)| \leq C\,e^{-\alpha(\xi+\eta)},$$
$$|P^{(2)}(\xi, \eta_*)| \leq C\,e^{-\alpha(\xi+\eta_*)}$$
$$|P^{(3)}(\xi_*, \eta_*)| \leq C\,e^{-\alpha(\xi_*+\eta_*)},$$
$$|P^{(4)}(\xi_*, \eta| \leq C\,e^{-\alpha(\xi_*+\eta)}.$$

From Boglayev [30], we have the following derivative estimates:

LEMMA 3.2 [30, Lemma 2]. Let $u(x, y) \in C^n(\bar{\Omega}) \cup C^{n+2}(\Omega)$ be the solution of the problem (79), (80). Then, the derivatives of u satisfy the following estimates:

$$\text{(I)} \quad |u_{x^n}(x, y)| \leq C_n(1 + \varepsilon^{-n} e^{(-\beta x)/\varepsilon} + \varepsilon^{-n} e^{(-\beta(1-x)/\varepsilon)}) \quad \text{on } \bar{\Omega},$$

$$\text{(II)} \quad |u_{y^n}(x, y)| \leq C_n(1 + \varepsilon^{-n} e^{(-\beta y)/\varepsilon} + \varepsilon^{-n} e^{(-\beta(1-y))/\varepsilon)}) \quad \text{on } \bar{\Omega},$$

where $0 < \beta < m_1^{1/2}$, and $n = 1, 2, 3$.

Since the problem (79), (80) has the same boundary layers as the linear one (3), (4), we can use the same piecewise uniform mesh as we constructed for the linear case.

The weak solution of (79), (80) is: Find $u \in H_0^1(\Omega)$ such that

$$\varepsilon^2(\nabla u, \nabla v) + (F(u, x, y), v) = 0, \quad \forall v \in H_0^1(\Omega). \tag{83}$$

The finite element solution is: Find $u_h \in S_h(\Omega)$ such that

$$\varepsilon^2(\nabla u_h, \nabla v_h) + (F(u_h, x, y), v_h) = 0, \quad \forall v_h \in S_h(\Omega), \tag{84}$$

where $S_h(\Omega)$ is the tensor–product quadratic element space used in last section.

Then, by carrying out the same proof as we did for the linear case, we can obtain the following interpolation estimate:

LEMMA 3.3. For the solution u of (79), (80) and any integer $n \geq 0$, we have

$$\|u - \Pi u\|_{\infty,\Omega} \leq C(N_x^{-3} \ln^3 N_x + N_y^{-3} \ln^3 N_y + \varepsilon^{n+1}).$$

Then, we have

THEOREM 3.1. Let u_h be the finite element solution of (84), and u be the analytic solution of (79), (80). Then, we have

$$\|u - u_h\| \leq C(1 + \varepsilon N_x + \varepsilon^{1/2} N_x \ln^{-1/2} N_x + \varepsilon N_y + \varepsilon^{1/2} N_y \ln^{-1/2} N_y)\|u - \Pi u\|_{\infty,\bar{\Omega}}.$$

PROOF. By subtracting (84) and (83), we have

$$\varepsilon^2(\nabla(u - u_h), \nabla v_h) + (F(u, x, y) - F(u_h, x, y), v_h) = 0, \quad \forall v_h \in S_h(\Omega) \tag{85}$$

By the mean value theorem, we can rewrite (85) as

$$\varepsilon^2(\nabla(u - u_h), \nabla v_h) + (\tilde{F}_u \cdot (u - u_h), v_h) = 0, \quad \forall v_h \in S_h(\Omega), \tag{86}$$

where $\tilde{F}_u$ denotes the value of the derivative F_u at some point $\theta u + (1 - \theta)u_h$, $0 < \theta < 1$.

From (86), we have

$$\varepsilon^2(\nabla(\Pi u - u_h), \nabla v_h) + (\tilde{F}_u \cdot (\Pi u - u_h), v_h) \tag{87}$$

$$= \varepsilon^2(\nabla(\Pi u - u), \nabla v_h) + (\tilde{F}_u \cdot (\Pi u - u), v_h), \quad \forall v_h \in S_h(\Omega). \tag{88}$$

By denoting $\chi = \Pi u - u_h$, choosing $v_h = \chi$ in (87), (88) and using the assumption (A2), we can obtain

$$\varepsilon^2\|\nabla\chi\|^2 + m_1\|\chi\|^2 \leq \varepsilon^2|(\nabla(\Pi u - u), \nabla\chi)| + |(\tilde{F}_u \cdot (\Pi u - u), \chi)| \tag{89}$$

The rest of proof can be carried in the same way as in Theorem 2.1. □

Under the assumption (A3), we can easily obtain the following quasi-optimal global uniformly convergent result:

THEOREM 3.2. Let u_h be the bi-quadratic finite element solution of (84) and u be the solution of (79), (80). Then, under the assumptions of (A1), (A2) and (A3), we have

$$\|u - u_h\| \leq C(N_x^{-3} \ln^3 N_x + N_y^{-3} \ln^3 N_y)\,, \tag{90}$$

where the constant C is independent of the perturbation parameter ε.

Similar results can be obtained for the mth order ($m \geq 3$) tensor–product element when there exists a smooth enough solution of (79), (80).

4. Numerical experiments

For simplicity, we only carried out our experiments for a linear problem by using the bi-quadratic element. Here we chose $N_x = N_y = N$ and tensor–product quadratic interpolation for the functions a and f in our numerical experiments. In Figs. 1–21, we always use (a) for the left figure and (b) for the right figure.

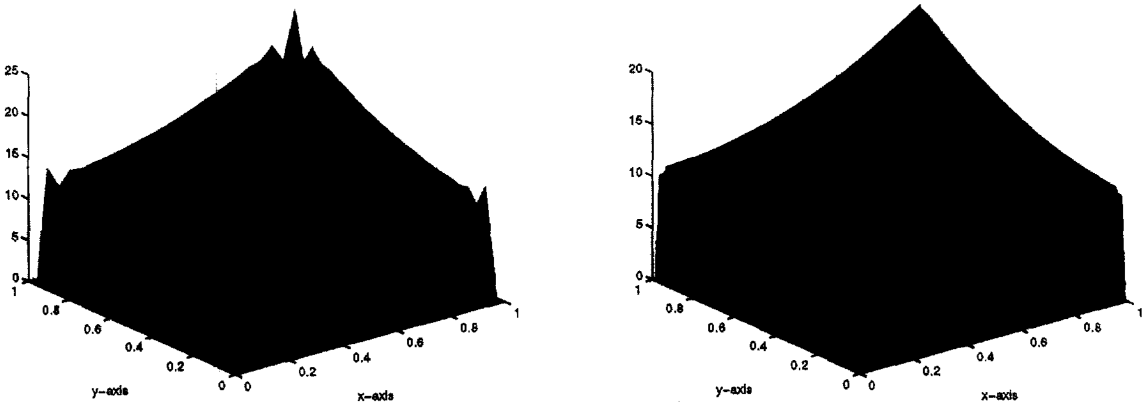

Fig. 1. Example 1: Computed FEM solution for $N = 12$ and $\varepsilon = 10^{-2}$. (a) Uniform mesh; (b) piecewise uniform mesh.

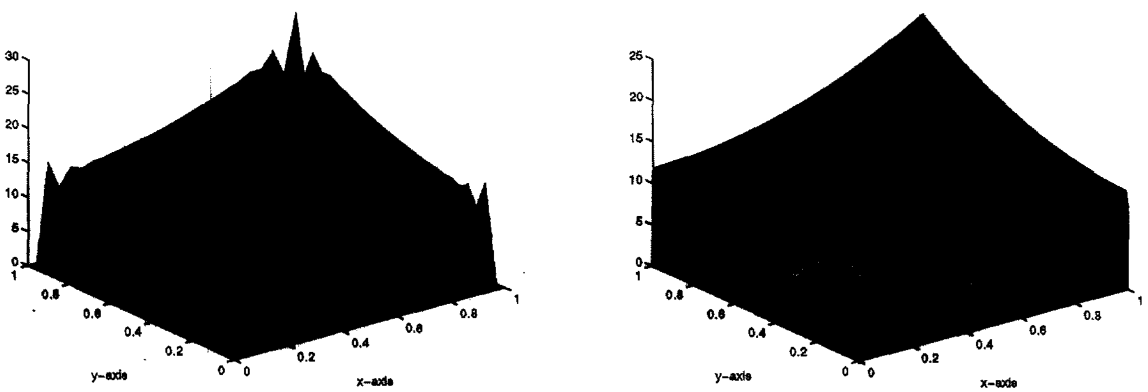

Fig. 2. Example 1: Computed FEM solution for $N = 12$ and $\varepsilon = 10^{-3}$. (a) Uniform mesh; (b) piecewise uniform mesh.

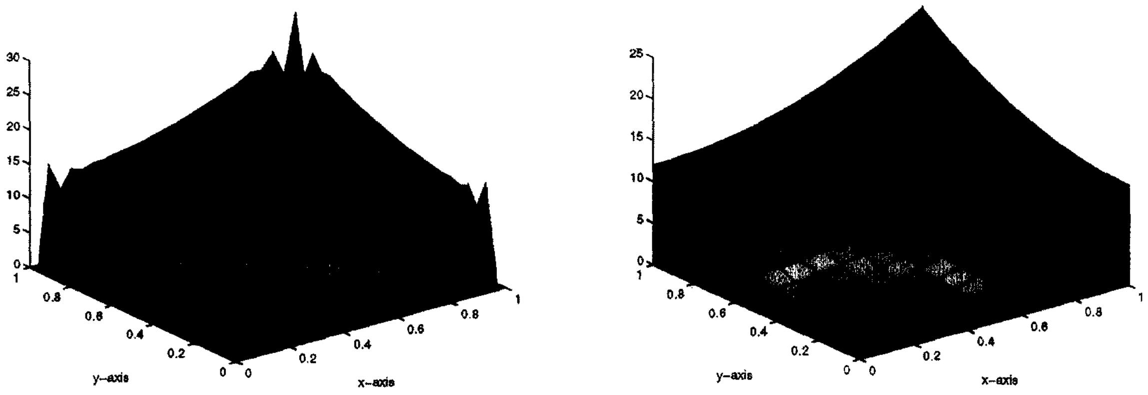

Fig. 3. Example 1: Computed FEM solution for $N = 12$ and $\varepsilon = 10^{-4}$. (a) Uniform mesh; (b) piecewise uniform mesh.

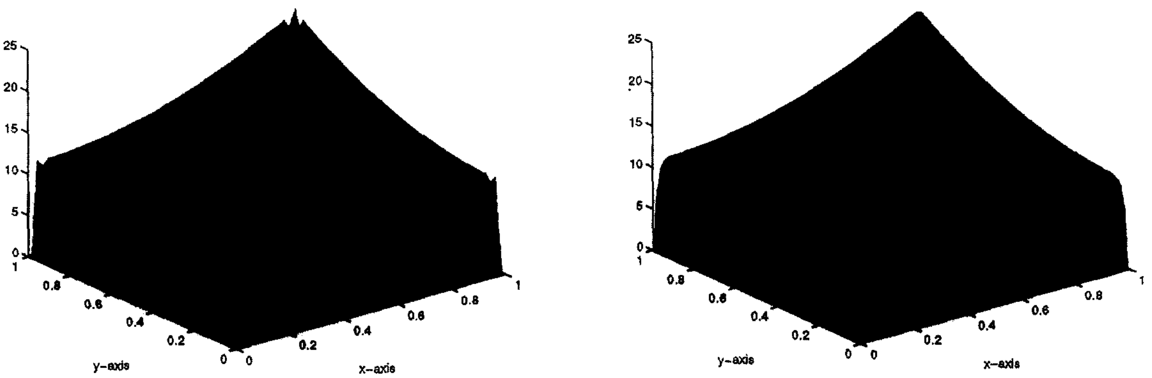

Fig. 4. Example 1: Computed FEM solution for $N = 24$ and $\varepsilon = 10^{-2}$. (a) Uniform mesh; (b) piecewise uniform mesh.

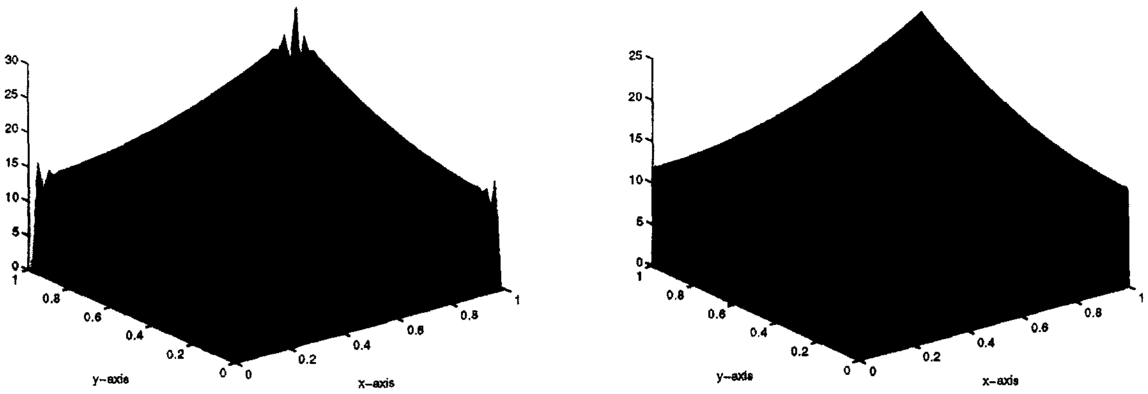

Fig. 5. Example 1: Computed FEM solution for $N = 24$ and $\varepsilon = 10^{-3}$. (a) Uniform mesh; (b) piecewise uniform mesh.

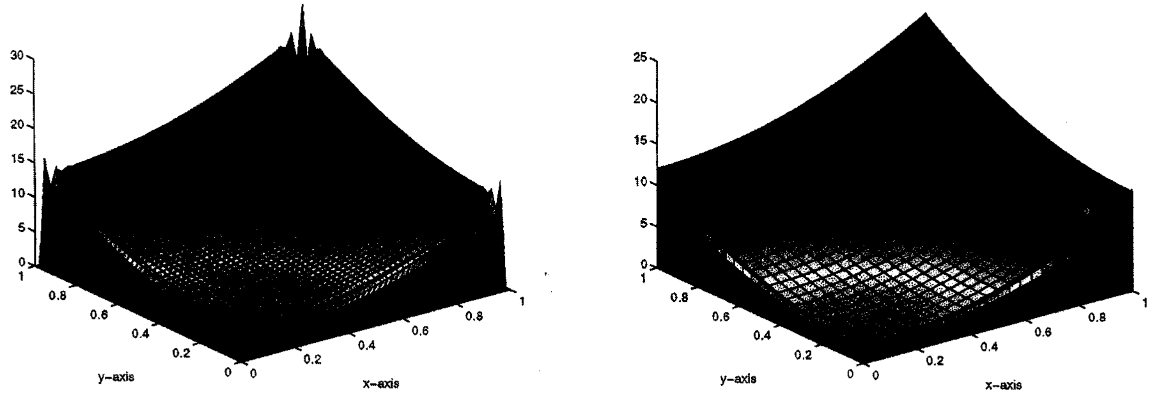

Fig. 6. Example 1: Computed FEM solution for $N = 24$ and $\varepsilon = 10^{-4}$. (a) Uniform mesh; (b) piecewise uniform mesh.

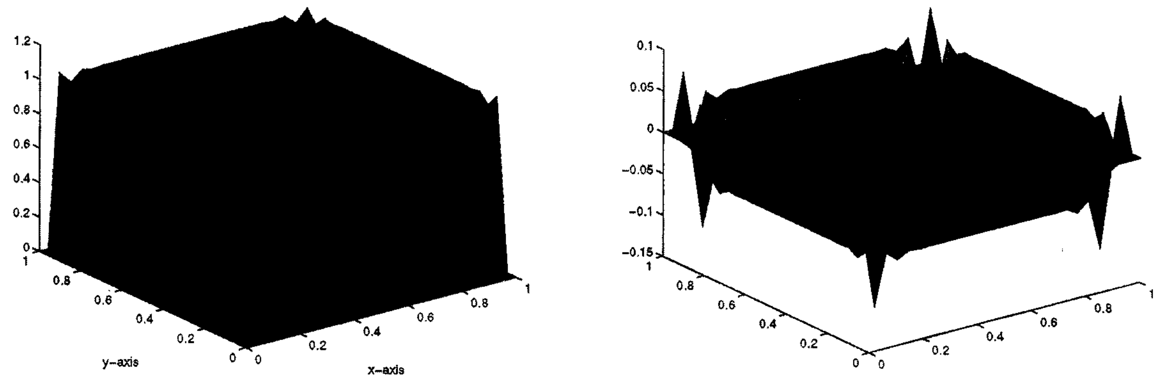

Fig. 7. Example 2: Standard FEM on uniform mesh with $N = 12$ and $\varepsilon = 10^{-2}$. (a) Computed solution; (b) pointwise error $u_h - u$.

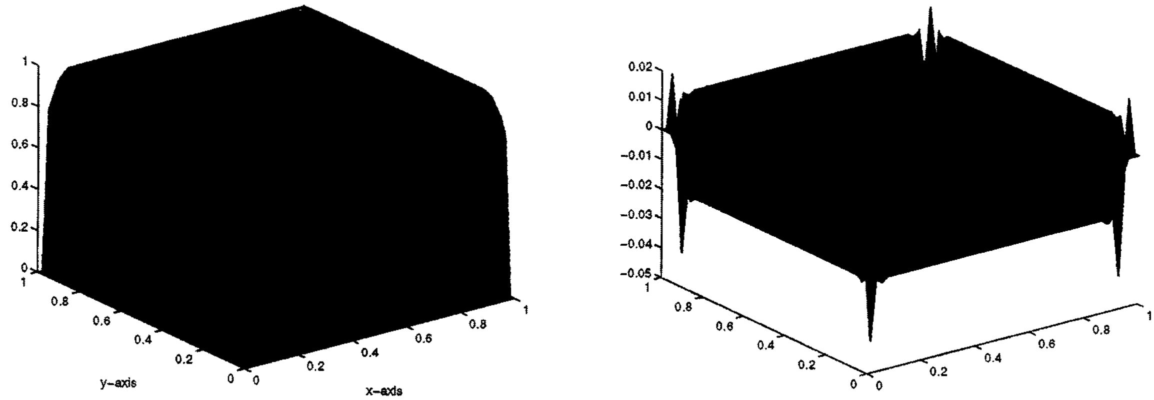

Fig. 8. Example 2: Standard FEM on uniform mesh with $N = 24$ and $\varepsilon = 10^{-2}$. (a) Computed solution; (b) pointwise error $u_h - u$.

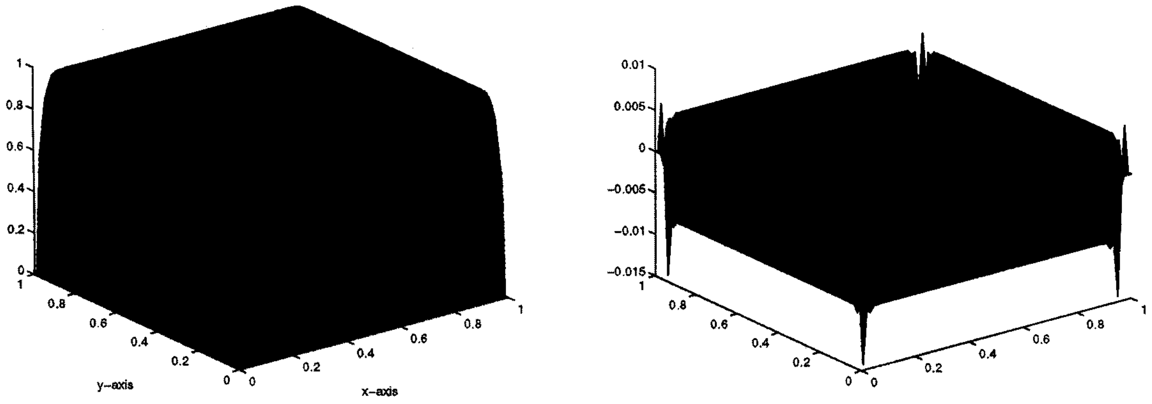

Fig. 9. Example 2: Standard FEM on uniform mesh with $N = 36$ and $\varepsilon = 10^{-2}$. (a) Computed solution; (b) pointwise error $u_h - u$.

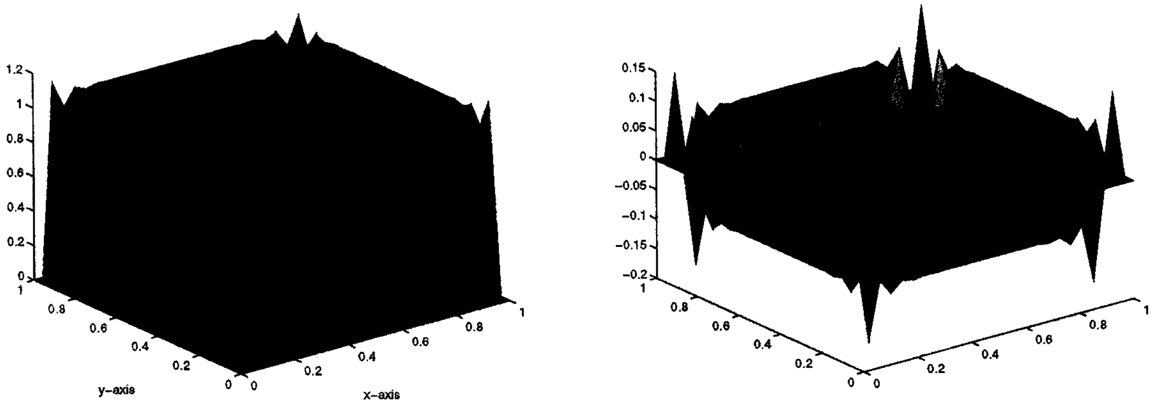

Fig. 10. Example 2: Standard FEM on uniform mesh with $N = 12$ and $\varepsilon = 10^{-3}$. (a) Computed solution; (b) pointwise error $u_h - u$.

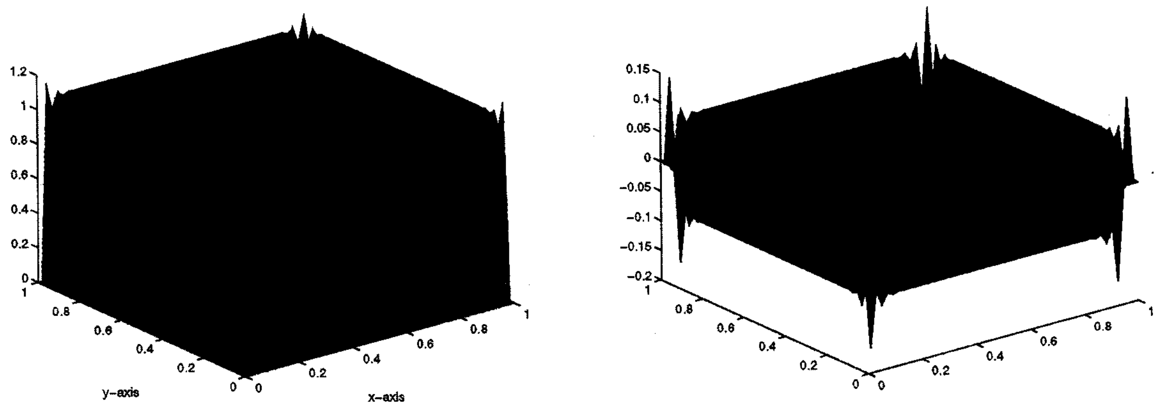

Fig. 11. Example 2: Standard FEM on uniform mesh with $N = 24$ and $\varepsilon = 10^{-3}$. (a) Computed solution; (b) pointwise error $u_h - u$.

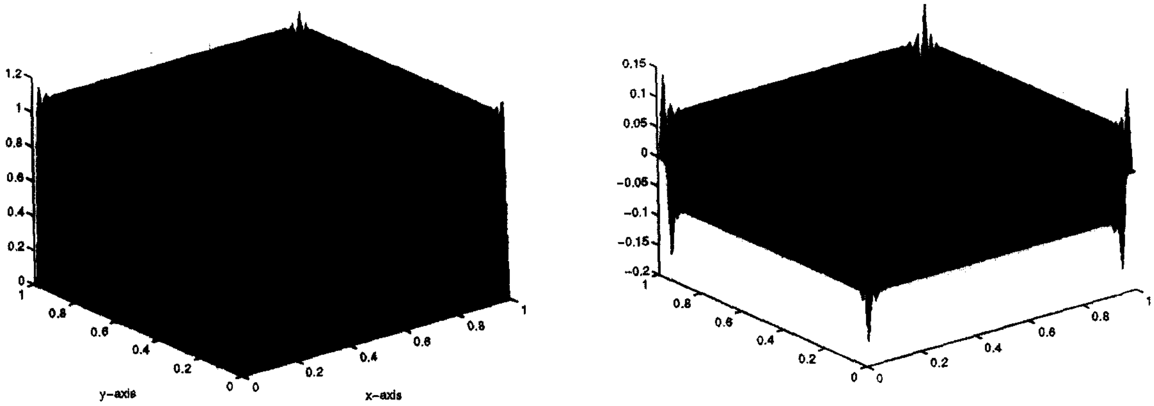

Fig. 12. Example 2: Standard FEM on uniform mesh with $N = 36$ and $\varepsilon = 10^{-3}$. (a) Computed solution; (b) pointwise error $u_h - u$.

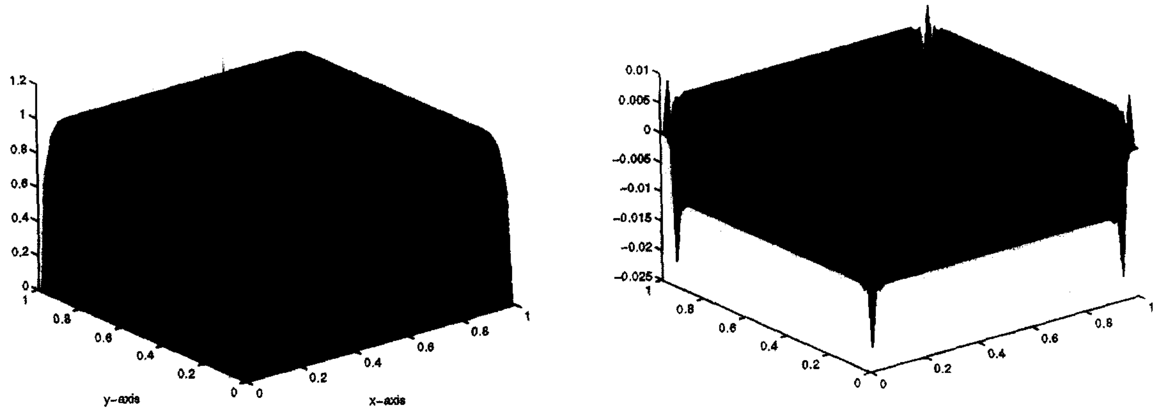

Fig. 13. Example 2: FEM on piecewise uniform mesh with $N = 12$ and $\varepsilon = 10^{-2}$. (a) Computed solution; (b) pointwise error $u_h - u$.

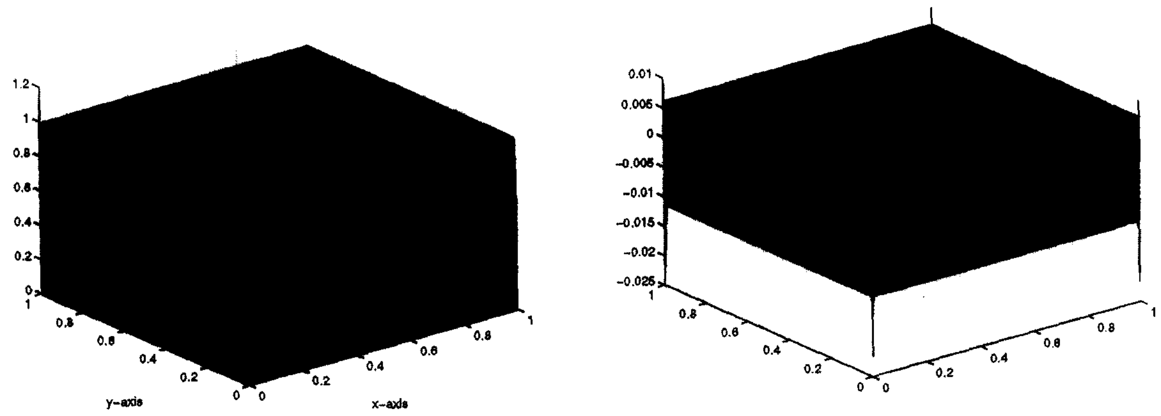

Fig. 14. Example 2: FEM on piecewise uniform mesh with $N = 12$ and $\varepsilon = 10^{-3}$. (a) Computed solution; (b) pointwise error $u_h - u$.

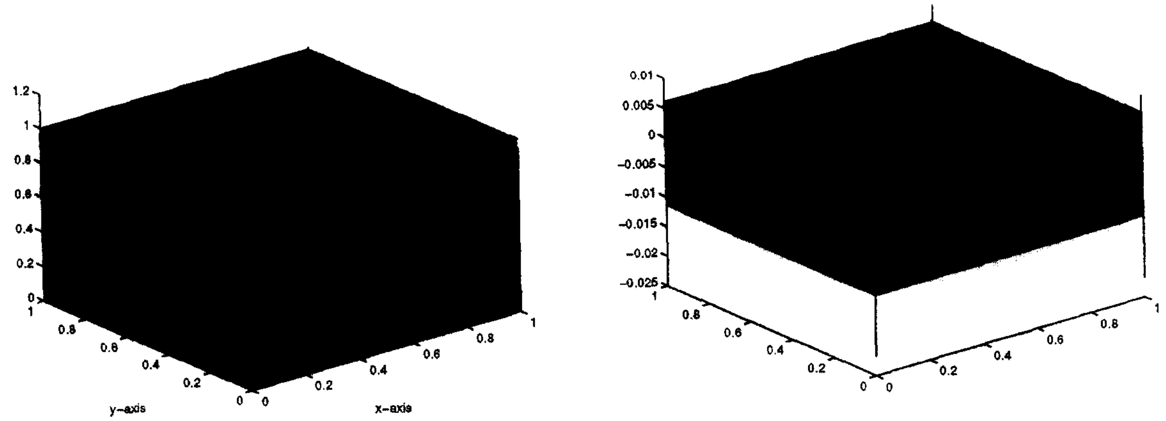

Fig. 15. Example 2: FEM on piecewise uniform mesh with $N = 12$ and $\varepsilon = 10^{-4}$. (a) Computed solution; (b) pointwise error $u_h - u$.

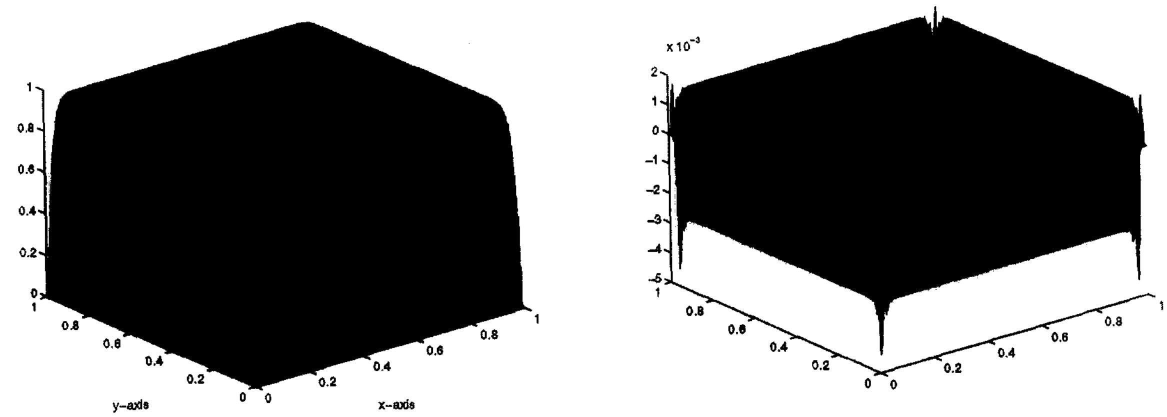

Fig. 16. Example 2: FEM on piecewise uniform mesh with $N = 24$ and $\varepsilon = 10^{-2}$. (a) Computed solution; (b) pointwise error $u_h - u$.

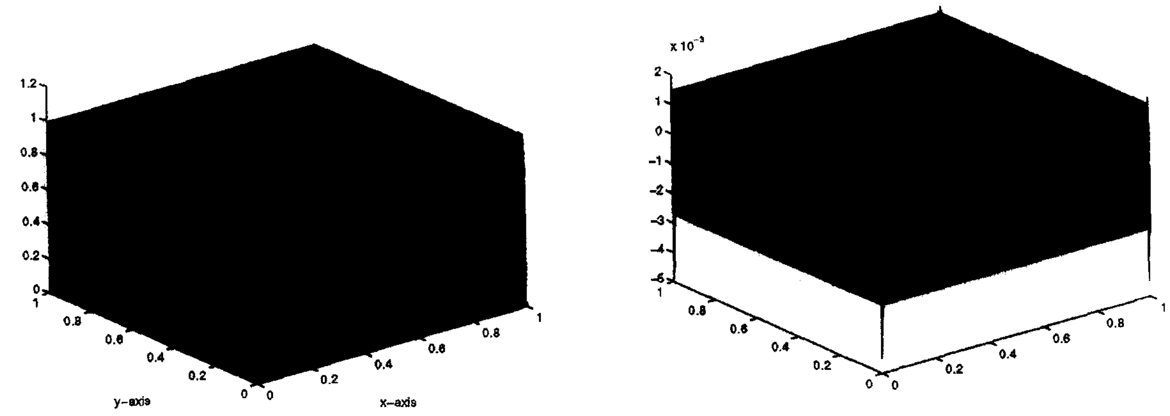

Fig. 17. Example 2: FEM on piecewise uniform mesh with $N = 24$ and $\varepsilon = 10^{-3}$. (a) Computed solution; (b) pointwise error $u_h - u$.

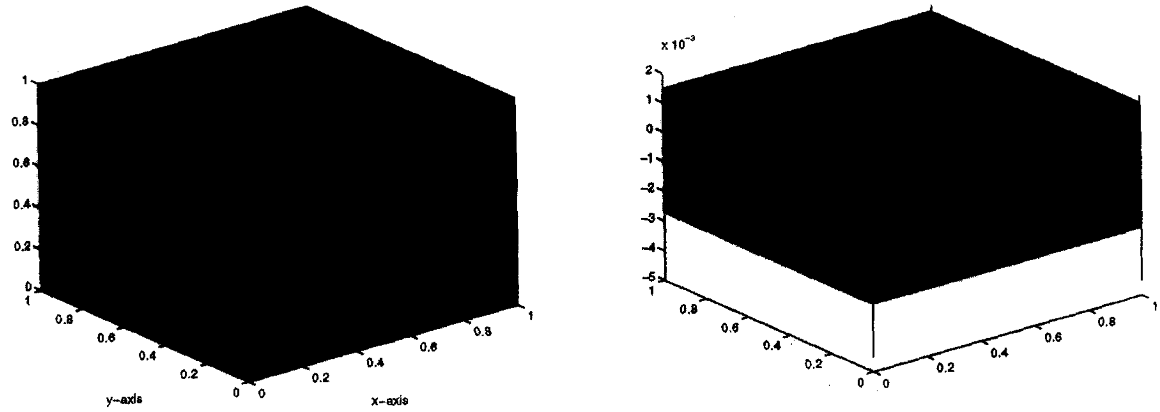

Fig. 18. Example 2: FEM on piecewise uniform mesh with $N = 24$ and $\varepsilon = 10^{-4}$. (a) Computed solution; (b) pointwise error $u_h - u$.

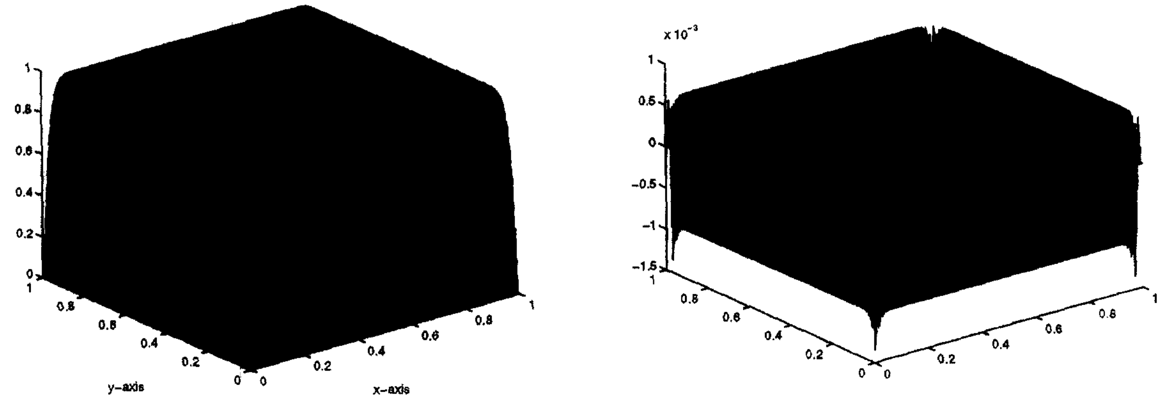

Fig. 19. Example 2: FEM on piecewise uniform mesh with $N = 36$ and $\varepsilon = 10^{-2}$. (a) Computed solution; (b) pointwise error $u_h - u$.

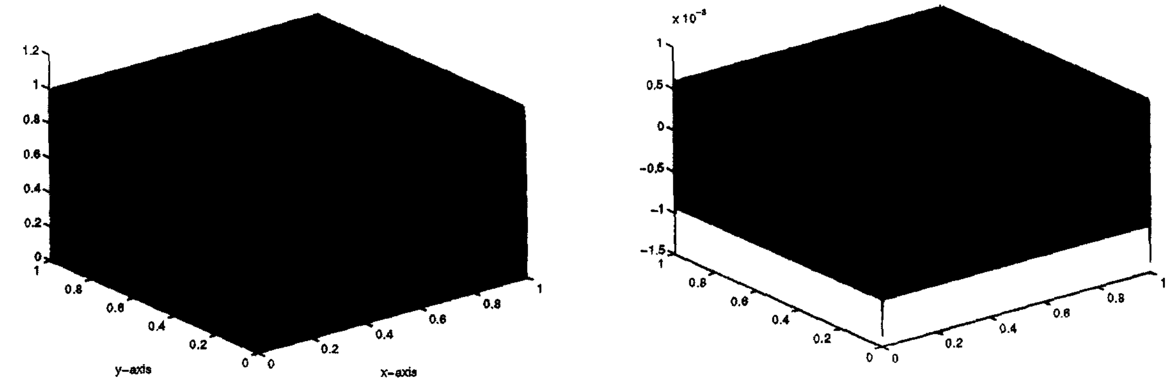

Fig. 20. Example 2: FEM on piecewise uniform mesh with $N = 36$ and $\varepsilon = 10^{-4}$. (a) Computed solution; (b) pointwise error $u_h - u$.

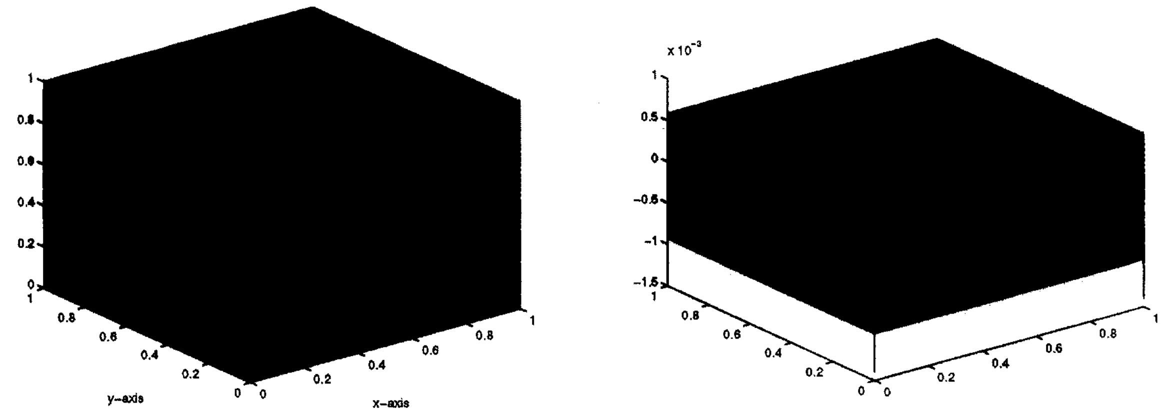

Fig. 21. Example 2: FEM on piecewise uniform mesh with $N = 36$ and $\varepsilon = 10^{-4}$. (a) Computed solution; (b) pointwise error $u_h - u$.

To see how our method performs, we first tested:

$$\text{Example 1:} \quad a = 2, f = 20(x^2 + y^2) + 4$$

on a uniform mesh and our piecewise uniform mesh for $N = 12$, 24 with different values of ε ranging from 10^{-7} to 10^{-2}. The computed solutions are presented in Figs. 1–6. These figures clearly show that our piecewise uniform mesh performs much better than the uniform mesh. Our piecewise uniform mesh resolves the sharp boundary layers without any oscillations. As ε decreases, the boundary layers become sharper. However, the finite element solution on our piecewise uniform mesh captures well the sharper layer. For $\varepsilon \leqslant 10^{-4}$, there is almost no distinction from the case of $\varepsilon = 10^{-4}$. On the other hand, the solutions achieved on the uniform mesh display wild oscillations near the boundary layers.

Note that $u_0 = 10(x^2 + y^2) + 2$ is the solution of the reduced problem (when $\varepsilon = 0$), so we know how the solution should look like.

To measure the accuracy of our method, we tested another case where $a = 2$, and f is chosen appropriately such that the exact solution is known:

$$\text{Example 2:} \quad u(x, y) = \left(1 - \frac{e^{-x/\varepsilon} + e^{-(1-x)/\varepsilon}}{1 + e^{-1/\varepsilon}}\right)\left(1 - \frac{e^{-y/\varepsilon} + e^{-(1-y)/\varepsilon}}{1 + e^{-1/\varepsilon}}\right)$$

The computed solution u_h and the pointwise error $u_h - u$ are shown in Figs. 7–12 for uniform mesh case, in Figs. 13–21 for piecewise uniform mesh case, respectively. The errors in L^2 norm on both meshes are provided in Tables 1 and 2, respectively, from which the uniform convergence in both cases is displayed very clearly. The estimated convergence rates

$$R = (\ln(e_{N_1}/e_{N_2}))/\ln(N_2/N_1) \quad \text{and} \quad \tilde{R} = (\ln(e_{N_1}/e_{N_2}))/\ln((N_2 \ln N_1)/(N_1 \ln N_2))$$

are displayed in Tables 3 and 4 for uniform mesh and piecewise uniform mesh, respectively. Here e_N is the L^2

Table 1
Errors in L^2 norm for Example 2 on uniform mesh

ε	N		
	12	24	36
1.0D-02	5.343611226D-03	1.491899416D-03	4.792132997D-04
1.0D-03	8.248501599D-03	5.681738618D-03	4.510826979D-03
1.0D-04	8.287975532D-03	5.791569840D-03	4.708982201D-03
1.0D-05	8.288371573D-03	5.792682315D-03	4.711020991D-03
1.0D-06	8.288375523D-03	5.792693454D-03	4.711041357D-03
1.0D-07	8.288375743D-03	5.792693695D-03	4.711043842D-03

Table 2
Errors in L^2 norm for Example 2 on piecewise uniform mesh

ε	N		
	12	24	36
1.0D-02	4.502200765D-04	9.529793001D-05	3.150367818D-05
1.0D-03	4.498835982D-04	9.528746525D-05	3.150143528D-05
1.0D-04	4.498482216D-04	9.539294103D-05	3.364966957D-05
1.0D-05	4.499431756D-04	9.541306516D-05	3.365684243D-05
1.0D-06	4.499855183D-04	9.546553209D-05	3.367834599D-05
1.0D-07	4.501197773D-04	9.550416942D-05	3.369497776D-05

Table 3
Convergence rates R in L^2 norm on uniform mesh

ε	N	
	12	24
1.0D-02	1.8407	2.8009
1.0D-03	0.5378	0.5692
1.0D-04	0.5171	0.5104
1.0D-05	0.5169	0.5098
1.0D-06	0.5169	0.5098
1.0D-07	0.5169	0.5098

Table 4
Convergence rates $\tilde{R}$ in L^2 norm on piecewise uniform mesh

ε	N	
	12	24
1.0D-02	3.4728	3.8786
1.0D-03	3.4714	3.8784
1.0D-04	3.4687	3.6512
1.0D-05	3.4687	3.6512
1.0D-06	3.4677	3.6508
1.0D-07	3.4675	3.6505

error between the exact solution u and the computed solution u_h on a mesh with N partitions in both the x- and y-directions. Table 3 shows the uniform convergence rate of $O(h^{1/2})$, which agrees with the theoretical analysis of Schatz and Wahlbin [31, Theorem A.2]. Table 4 shows a better uniform convergence rate than our theoretically predicted rate. Note that Figs. 7(b)–12(b) show that the standard FEM on uniform mesh does not converge in L^∞ norm, while the standard FEM on our piecewise uniform mesh seems to be uniformly convergent in $L\infty$ norm. The pointwise error $u_h - u$ in Figs. 13(b)–21(b) decreases as N increases, and the error is dominated by that occurring at the four corners of the domain.

5. Conclusions

In this paper, we developed a general higher-order finite element method for solving the singularly perturbed elliptic linear and quasilinear problems in two space dimensions. The quasioptimal global uniform convergence rate $O(N_x^{-(m+1)} \ln^{m+1} N_x + N_y^{-(m+1)} \ln^{m+1} N_y)$ in L^2 norm was proved for solving the reaction–diffusion model by using the mth order ($m \geq 2$) tensor–product element, which answers part of Roos' open problems proposed in 1997 in [1] as we mentioned in the Introduction. Our numerical results also show the global uniform convergence in L^∞ norm, the proof of which is unavailable at present. Further investigation is required to address this issue.

From our proof, we can expect that our method can be directly applied to other singularly perturbed problems, which have similar asymptotic expansions and smooth enough solutions. Even though 'a posteriori' adaptive FEM sounds more promising for those SPP without an explicit asymptotic expansions, the task is more challenging. Though some effort has been done [32–36,14,18,17] in this direction, '*even from the practical point of view the existing adaptive strategies so far are not completely satisfactory*' [1, p. 306], since '*the construction of robust estimators is still an open problem*' [1, p. 306]. Only recently did Verfürth [33] obtain theoretically robust a posteriori error estimators, which are independent of the perturbation parameter, for the reaction–diffusion model, however without any implementation. Hence, to solve the singularly perturbed problems, a better strategy is to start the numerical computation with such a layer-adapted piecewise uniform mesh, and then to refine the mesh adaptively based on some robust error estimators [1]. Also, it would be very interesting if such a piecewise uniform mesh is implemented with the *hp*-FEM [14,18,17].

Acknowledgments

The first author wishes to thank Professors H.-G. Roos and L.F. Greengard for kindly providing references [1] and [35], respectively. The research of the authors was partly supported by the AFOSR under Grant F49620-96-1-0172.

References

[1] H.-G. Roos, Layer-adapted grids for singular perturbation problems, Z. Angew. Math. Mech, 78(5) (1998) 291–309.
[2] H.-G. Roos, M. Stynes and L. Tobiska, Numerical Methods for Singularly Perturbed Differential Equations (Springer-Verlag, Berlin, 1996).
[3] J.J.H. Miller, E. O'Riordan and G.I. Shishkin, Fitted Numerical Methods for Singular Perturbation Problems (World Scientific, Singapore, 1995).
[4] K.W. Morton, Numerical Solution of Convection–Diffusion Problems (Chapman and Hall, 1996).
[5] A.B. Vasil'eva, V.F. Butuzov and L.V. Kalachev, The Boundary Function Method for Singular Perturbation Problems (SIAM, Philadelphia, 1995).
[6] C.C. Lin and L.A. Segel, Mathematics Applied to Deterministic Problems in the Natural Sciences (SIAM, Philadelphia, 1988).
[7] M. Van Dyke, Perturbation Methods in Fluid Mechanics (Academic Press, New York, 1964).
[8] J.L. Lions, Perturbations Singulieres dans les Problemes aux Limites et en Controle Optimal (Springer-Verlag, Berlin, 1973).
[9] D.S. Naidu and A.K. Rao, Singular Perturbation Analysis of Discrete Control Systems (Springer-Verlag, New York, 1985).
[10] R. O'Malley, Singular Perturbations Methods for Ordinary Differential Equations (Springer-Verlag, New York, 1991).
[11] G.F. Carey and J.T. Oden, Finite Elements: Fluid Mechanics, Vol. VI (Prentice-Hall, Englewood Cliffs, NJ, 1986).
[12] O.C. Zienkiewicz and R.L. Taylor, The Finite Element Method, Vol. 2 (McGraw-Hill Publ., New York, 1991).
[13] T.J.R. Hughes, ed., Finite Element Methods for Convection-Dominated Flows, ASME Monograph AMD-34 (ASME, New York, 1979).
[14] J.T. Oden, Optimal *h-p* finite element methods, Comput. Methods Appl. Mech. Engrg. 112 (1994) 309–331.
[15] P.W. Hemker, A Numerical Study of Stiff Two-Point Boundary Value Problems (Mathematical Center, Amsterdam, 1977).
[16] H.-G. Roos, D. Adam and A. Felgenhauer, A novel nonconforming uniformly convergent finite element method in two dimensions, J. Math. Anal. Appl. 201 (1996) 715–755.
[17] C. Schwab and M. Suri, The *p* and *hp* versions of the finite element method for problems with boundary layers, Math. Comput. 65 (1996) 1403–1429.
[18] C. Schwab, M. Suri and C. Xenophontos, The *hp* finite element method for problems in mechanics with boundary layers, Technical Report 96-14, Department of Mathematics & Statistics, University of Maryland Baltimore County, December 1996.
[19] G.I. Shishkin, Grid approximation of singularly perturbed parabolic equations with internal layers, Russian J. Numer. Anal. Math. Model. 3 (1988) 393–407.
[20] M. Stynes and E. O'Riordan, A uniformly convergent Galerkin method on a Shishkin mesh for a convection–diffusion problem, J. Math. Anal. Appl. 214 (1997) 36–54.
[21] J. Li, Quasi-optimal uniformly convergent finite element methods for the elliptic boundary layer problem, Comput. Math. Applic. (33)10 (1997) 11–22.
[22] J. Li and I.M. Navon, Uniformly convergent finite element methods for singularly perturbed elliptic boundary value problems I: reaction–diffusion type, Comput. Math. Applic. (35)3 (1998) 57–70.
[23] J. Li and I.M. Navon, Uniformly convergent finite element methods for singularly perturbed elliptic boundary value problems II: convection–diffusion type, Comput. Methods Appl. Mech. Engrg. 162 (1998) 49–78.
[24] J. Li and I.M. Navon, A global uniformly convergent finite element method for a quasilinear singularly perturbed elliptic problem, SCRI-98T-14, Florida State University, 1998.

[25] H. Han and R.B. Kellogg, Differentiability properties of solutions of the equation $-\varepsilon^2 \Delta u + ru = f(x, y)$ in a square, SIAM J. Math. Anal. 21 (1990) 394–408.

[26] V.F. Butuzov, The asymptotic properties of solutions of the equation $\mu^2 \Delta u - k^2(x, y)u = f(x, y)$ in a rectangle, Differential Eqs. 9 (1973) 1274–1279.

[27] E.B. Becker, G.F. Carey and J.T. Oden, Finite Elements: An Introduction, Vol. I (Prentice-Hall, Englewood Cliffs, NJ, 1981).

[28] S.C. Brenner and L.R. Scott, The Mathematical Theory of Finite Element Methods (Springer-Verlag, New York, 1994).

[29] I.V. Denisov, Quasilinear singularly perturbed elliptic equations in a rectangle, Comput. Math. Math. Phys. 35 (1995) 1341–1350.

[30] I.P. Boglayev, A numerical method for solving quasilinear elliptic equations with a small parameter for the highest derivatives, Comput. Math. Math. Phys. 28 (1988) 118–125.

[31] A.H. Schatz and L.B. Wahlbin, On the finite element method for singularly perturbed reaction–diffusion problems in two and one dimensions, Math. Comput. 40 (1983) 47–89.

[32] W.G. Szymczak and I. Babǔska, Adaptivity and error estimation for the finite element method applied to convection diffusion problem, SIAM J. Numer. Anal. 21 (1984) 910–953.

[33] R. Verfürth, Robust a posteriori error estimators for a singularly perturbed reaction–diffusion equation, Numer. Math. 78 (1998) 479–493.

[34] H.-J. Reinhardt, A posteriori error estimates for the finite element solution of a singularly perturbed linear ordinary differential equation, SIAM J. Numer. Anal. 18 (1981) 406–430.

[35] J.-Y. Lee, Adaptive numerical methods for singular perturbation problems in one space dimension, Ph.D. Dissertation, Courant Institute of Mathematical Sciences, 1994.

[36] L. Demkowicz and J.T. Oden, An adaptive characteristic Petrov–Galerkin finite element method for convection-dominated linear and nonlinear parabolic problems in one space variable, J. Comput. Phys. 67 (1986) 188–213.